Invited Paper

Progress and issues for high speed vertical cavity surface emitting lasers

Kevin L. Lear[a*] and Ahmad N. Al-Omari[b]
[a]Colorado State University, Electrical and Computer Engineering Department
MS 1373, Fort Collins, CO, USA 80523-1373
[b]Yarmouk University, Hijjawi Faculty, Electronic Engineering Department, Irbid, Jordan 21163

ABSTRACT

Extrinsic electrical, thermal, and optical issues rather than intrinsic factors currently constrain the maximum bandwidth of directly modulated vertical cavity surface emitting lasers (VCSELs). Intrinsic limits based on resonance frequency, damping, and K-factor analysis are summarized. Previous reports are used to compare parasitic circuit values and electrical 3dB bandwidths and thermal resistances. A correlation between multimode operation and junction heating with bandwidth saturation is presented. The extrinsic factors motivate modified bottom-emitting structures with no electrical pads, small mesas, copper plated heatsinks, and uniform current injection. Selected results on high speed quantum well and quantum dot VCSELs at 850 nm, 980 nm, and 1070 nm are reviewed including small-signal 3dB frequencies up to 21.5 GHz and bit rates up to 30 Gb/s.

Keywords: VCSEL, laser diode modulation, frequency response, thermal impedance, RC time constants

1. INTRODUCTION

The relative low manufacturing cost, high performance, and simplified systems integration of vertical cavity surface emitting lasers (VCSELs) have driven them to dominate short haul data communication applications such as Gigabit Ethernet. Arrays of these lasers are even more attractive for high aggregate bandwidth systems based on parallel fibers or waveguides. While VCSELs operating at 10 Gb/s are commercially available, higher bandwidths are needed to outpace the capabilities of copper in applications such as chip-to-chip optical interconnects. Especially in very short distance interconnects of < 1m, directly modulated VCSELs are the bandwidth bottleneck. Significantly increased modulation bandwidth can be achieved with optical injection biasing [1] or external modulation [2], but direct modulation is particularly attractive to maintain simplified electrical, mechanical, and optical system interfaces.

Research indicates that faster directly modulated VCSEL data rates are possible, but a number of factors must be addressed to realize the full potential of this approach. Work performed a decade or more ago establishes intrinsic modulation bandwidths are in excess of 50 GHz. High current pulsed VCSEL measurements exhibited relaxation oscillations of 70 GHz [3]. Standard extrapolation analysis of damping rate dependence on resonant frequency, discussed below, projected critically damped 3dB bandwidths of 57 GHz [4]. Directly modulated Fabry-Perot edge emitting lasers based on highly strained InGaAs operating at 1070 nm have reached bandwidths near 40 GHz in devices with intrinsic bandwidth limits of approximately 37 GHz [5]. However, extrinsic factors including parasitic circuit elements, high junction temperatures, and multi-mode operation have prevented VCSELs from reaching their intrinsic capabilities. Section 2 presents an overview of these factors before selected VCSEL modulation results are summarized in Section 3. The authors' work on structures addressing the limiting factors is reviewed in Section 4 before the paper's summary in Section 5.

* Email: KLLear@engr.colostate.edu; website: www.engr.colostate.edu/~kllear

Vertical-Cavity Surface-Emitting Lasers XI, edited by Kent D. Choquette, James K. Guenter,
Proc. of SPIE Vol. 6484, 64840J, (2007) · 0277-786X/07/$18 · doi: 10.1117/12.715081

2. VCSEL MODULATION ISSUES

2.1 Intrinsic bandwidth

Photons and electronic carriers, electrons and holes, are interacting energy storage mechanisms in laser diodes that give rise to relaxation oscillations. The rate equations for photons and carriers include non-linear terms, specifically the product of carrier concentration dependent gain with photon density, but can be linearized to yield a small-signal damped oscillator model with a frequency response given by $H(\omega) = \omega_R^2/(\omega_R^2-\omega^2+i\omega\gamma)$ where ω is the angular frequency, $\omega_R = [(dg/dn)_{th}s_{avg}v_g/\tau_{ph}]^{1/2}$ is the resonant angular frequency which depends on the differential modal gain at threshold, $(dg/dn)_{th}$, the average photon density, s_{avg}, the photon group velocity, v_g, and the cavity's photon lifetime, τ_{ph}. Since the laser's output power, P, is proportional to the photon density, the resonance frequency is ideally proportional to $P^{1/2}$, as illustrated in Fig. 1(a). The damping constant is $\gamma = 1/\tau_n+\omega_R^2\tau_{ph}[1+\varepsilon\Gamma g/(dg/dn)_{th}] = \gamma_0+Kf_R^2$ and represents the rate of energy loss due to the differential carrier lifetime in the absence of stimulated emission, τ_n, as well as optical losses where ε is the gain compression coefficient and Γ is the confinement factor. Note that the damping constant increases linearly with laser power, P, or quadratically with the resonance frequency as shown in Fig. 1(a). In practice, the damping coefficient at threshold, γ_0, and the damping parameter, K, are empirically determined from fitting the measured frequency response to obtain ω_R and γ for various bias currents above threshold. When the resonant frequency reaches $f_R = \gamma/(8\pi^2)^{1/2}$ the system becomes critically damped and the ultimate intrinsic bandwidth can be approximated as $f_{3dB,max} = (8\pi^2)^{1/2}/K$ if $\gamma_0/2\pi f_R$ is negligible, although this is not the case in some of the following data. The observed maximum bandwidths of various VCSELs discussed in Section 3 fall well below the maximum intrinsic bandwidths due to extrinsic limitations associated with parasitic circuit elements, excessive heating in the junction, and multimode operation. These three extrinsic factors are discussed in the following three subsections.

The preceding equations are based on a small-signal linear treatment of the laser diode rate equations. However, many data communication systems require a sufficiently large extinction ratio that non-linear factors need to be considered. This paper does not specifically address these large signal non-linear effects, but care should be used in predicting maximum bit rates from small signal bandwidths if large extinction ratios are required.

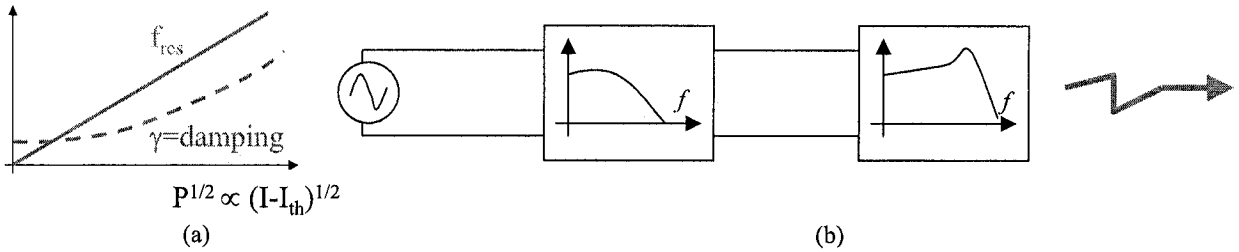

(a) (b)

Fig. 1. (a) Functional dependence of resonant frequency and damping rate on the square root of laser power. Damping rate is quadratically related to the resonant frequency. (b) Electrical network representation of a laser diode system with an intrinsic resonant filter response on the right preceded by a low pass electrical system due to undesired parasitic circuit elements as discussed in Subsection 2.2.

2.2 External parasitic circuit limitations

The laser diode frequency response described above represents the intrinsic behavior of the laser with respect to current that is injecting carriers that contribute to gain. Various phenomena including carrier transport, capture, escape, and confinement layer recombination affect what portion of the junction current contributes to gain and thus stimulated recombination, but will not be discussed in this paper. However, it is appropriate in this review to comment on parasitic circuit elements associated with the laser diode structure that impede the modulated signal from reaching the laser junction. The parasitic circuit elements form a low pass electrical filter as represented in Fig. 1(b) that limits the modulation efficiency of the junction current which in turn drives the intrinsic response of the laser. The electrical parasitic circuit components do not impose the major limitation on VCSEL modulation bandwidth if they are properly engineered.

Fig. 2 shows a schematic cross-section of an oxide-confined VCSEL mesa with an equivalent circuit superimposed on the features. Such a structure, used to realize 21.5 GHz VCSELs at Sandia National Laboratories in the mid 1990s as will be discussed in greater detail in Section 3, was the subject of circuit modeling[4]. It is desirable for the electrical

signal that is applied to the metal interconnect pads to generate as large of current modulation as possible through the active region represented by the resistor R_a. The capacitance of the combined oxide and perimeter junction, C_a, shunts high frequency current intended for R_a. In order to reduce the area contributing to this capacitance, a high energy proton implant was used to make the majority of the mesa insulating [4]. The series resistance of both the upper and lower mirror can be lumped into R_s for a simple model although R_a, C_a, and R_s, could all be considered as distributed components from a physical perspective. An additional shunt path is provided by the pad capacitance, C_p, where a resistance, R_p, has been included to properly match the experimentally observed loss associated with test pad capacitors not connected to laser mesas. This loss was initially attributed to the limited conductivity of the partially etched mirror below the polyimide, but has more recently been determined to mostly represent the dielectric loss of the polyimide [6]. Thick polyimide was sufficient to reduce the capacitance of the ~10000 μm^2 pad to 42 fF. Other approaches to reduced capacitance will be described in Sections 3 and 4. Low mirror resistances play an important role in reducing the RC time constants of parasitic circuits as well as increasing device efficiency that reduces laser heating. Researchers have investigated a number of heterojunction grading and modulation doping approaches for reducing VCSEL mirror resistance [7].

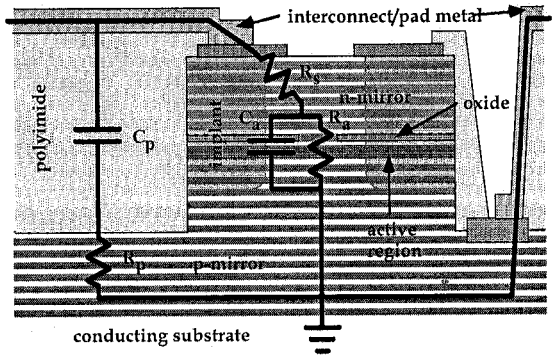

Fig. 2. Schematic cross-section of a oxide-confined VCSEL with superimposed circuit diagram. An implant has been used to reduce the capacitance, C_a, associated with the oxide and junction outside the active area. Reproduced from [4].

Table 1. Electrical circuit parameters including junction resistance (R_a), mesa capacitance(C_a), series mirror resistance (R_S), pad capacitance (C_p), and pad capacitor resistance (R_p) for high speed VCSELs reported by two research groups. These parameters correspond to the elements represented in Fig. 2 although some authors refer to them by other symbols or names. The open-circuit time constants for the mesa, τ_a, and pad, τ_p, are reported assuming a 50Ω driving source. The electrical 3dB frequency is calculated using the full equivalent circuit.

Research organization /reference		Active area /μm^2	R_a /Ω	C_a /fF	τ_a /ps	R_S /Ω	C_p /fF	R_p /Ω	τ_p /ps	Elec. f_{3dB} /GHz
Sandia [4]	oxide, low dose implant	4x4	120.4	152.1	7.38	31.3	41.7	15.9	2.23	18.8
Sandia [4]	oxide, medium dose implant	4x4	269.6	72.9	4.77	36.3	41.7	15.9	2.46	25.8
Sandia [4]	oxide, high dose implant	4x4	288.7	44.3	2.73	28.3	41.7	15.9	2.46	36.4
NEC [8]	oxide, implanted	$\pi 3.5^2$	104.7	145.0	6.66	31.9	56.0	0	2.05	20.2
NEC [8,9]	tunnel junction, no implant	$\pi 3^2$	62.1	280.0	9.87	31.5	33.0	0	1.08	15.3

Open-circuit time constant circuit analysis can be used to estimate the electrical 3dB bandwidth of the structure [10]. The time constant associated with the C_a is $\tau_a=C_a[R_a||(R_s+Z_0)]$ where $Z_0=50\Omega$ is the Thevenin equivalent resistance of the signal source. The time constant associated with C_p is $\tau_p=C_p[R_p+((R_s+R_a)||Z_0)]$. A conservative estimate of the electrical 3dB bandwidth is then $f_{3dB,elec}\approx[2\pi(\tau_a+\tau_p)]^{-1}$. Using the values reported in Reference [4] and listed in Table 1 with the largest implant dose, the electrical 3dB frequency is $f_{3dB,elec}$=36.4 GHz, showing that the VCSEL's 21.5 GHz bandwidth was not limited by electrical parasitic circuit components. However, high speed VCSELs can be parasitic limited as described in Section 4.

2.3 Thermal management

In order to reach the very high intrinsic damping limited bandwidths given in Section 2.1, the heat generated by the required drive levels must be appropriately managed. Excessive junction temperatures are observed to cause the resonant frequency to saturate, presumably due to the decrease in the threshold differential gain, $(dg/dn)_{th}$, as well as an increase in threshold current at higher gain region temperatures. Experiments such as those illustrated below in Fig. 3 have shown that reducing the ambient or case temperature results in higher absolute maximum bandwidths. In order to achieve higher bandwidths without active cooling, the VCSEL's thermal resistance must be lowered to reduce the temperature difference between the junction and device's case or heatsink. Multiple approaches for reducing thermal resistance are discussed in Section 4.

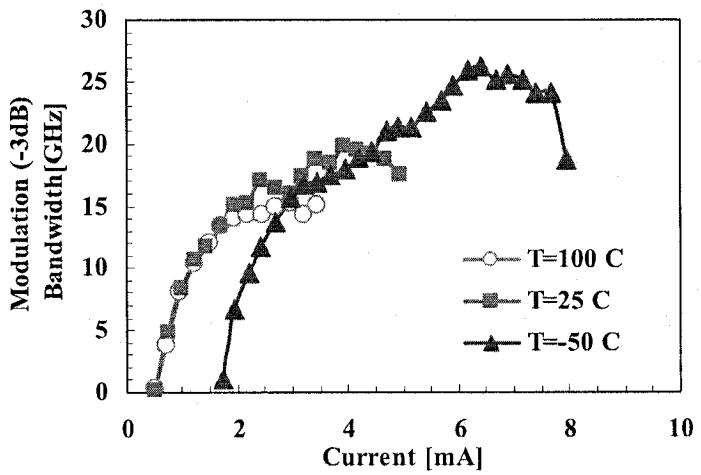

Fig. 3. Maximum 3dB bandwidth of an 850 nm oxide confined VCSEL as a function of bias current. Reproduced from [4].

2.4 Mode control

In addition to extrinsic electrical and thermal properties, optical behavior can also limit direct modulation bandwidths to values less than the theoretical intrinsic limits. Because the resonant frequency and thus bandwidth in the low damping limit grow in proportion $P^{1/2}$, i.e. to the square root of photon density, spreading photons among multiple mutually incoherent modes significantly impedes the increase in bandwidth. If the optical power is spread equally across N modes, then the bandwidth grows in proportion to $(P/N)^{1/2}$, in effect decreasing the MCEF by $N^{1/2}$. More often, the number of modes reaching threshold continues to increase with current so that bandwidth often saturates once the laser begins to operate in multiple modes. Fig. 4 shows the 3dB bandwidth of a high speed 850 nm VCSEL as a function of $(I-I_{th})^{1/2}$ with output spectra displayed corresponding to the different bias conditions [11]. Once the first higher order mode reaches a power level equal to that of the fundamental mode, which occurs at the longest wavelength, the bandwidth saturates and does not increase further with additional increases in bias. In order to obtain performance closer to the intrinsic limits of VCSELs, the lasers must be made to operate in a single, preferably highest photon density fundamental, mode to very high bias currents.

3. REVIEW OF MODULATION BANDWIDTH PROGRESS

A few important results from the historical development of high speed VCSELs as well as recent developments are summarized in this section.

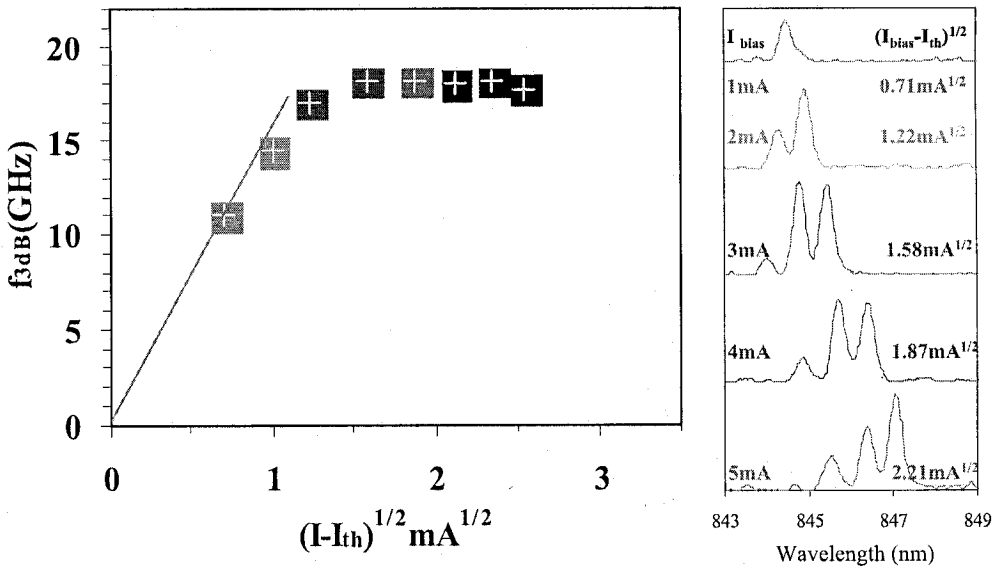

Fig. 4. 3dB bandwidth of an 850 nm oxide confined VCSEL along with output spectra showing that the laser has a dominant fundamental mode until I=3mA corresponding to $(I-I_{th})^{1/2} = 1.2\ mA^{1/2}$ at which point the bandwidth saturates.

3.1 Proton implanted VCSELs

Investigations of VCSEL dynamics shortly after proton implanted devices were first published placed the initial bandwidths in the 8 GHz range [12]. In 1993, Shtengel and co-authors at Colorado State University and Bandgap Technology Corp. reported a significant advance in the modulation rates of proton implanted VCSELs [13]. They were able to obtain maximum bandwidths of 10 GHz from 970 nm lasers and 14 GHz from 780 nm lasers. It is noteworthy that higher speeds were obtained from the shorter wavelength devices that did not benefit from strained InGaAs quantum wells and the associated expectation of higher differential gain occurring in the 970 nm active region. Shtengel et al's results remained the highest benchmarks for VCSEL bandwidth until the advent of oxide confined devices.

3.2 High bandwidth 850 nm oxide VCSELs

In 1997, one of the authors and colleagues at Sandia National Laboratories demonstrated direct modulation bandwidths up to 21.5 GHz in oxide confined, single mode 850 nm VCSELs [4,14]. The highest speed device that was measured had a threshold current of approximately 0.5 mA and differential resistance of 200 to 250 Ω as seen in Fig. 5(a). The

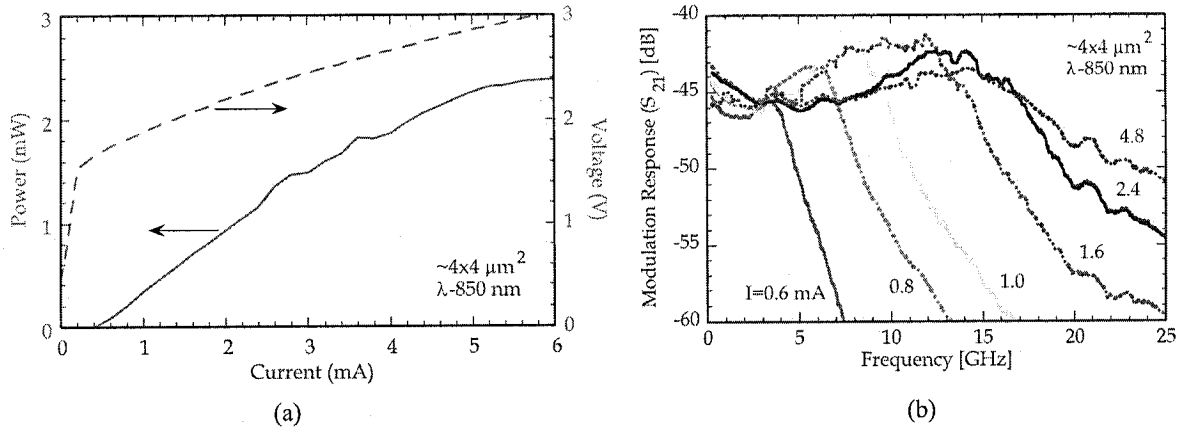

Fig. 5. (a) Output power and voltage versus drive current of a high speed, 850 nm, single mode, oxide confined VCSEL. (b) The measured microwave frequency response of the VCSEL at varying drive currents. Reproduced from [4].

bandwidth of the devices was enhanced by using proton implants to decrease the mesa capacitance as indicated in Fig. 2 and Table 1. The progression of 3dB bandwidth as well as the resonance frequency and damping coefficients obtained from fitting the frequency response data are shown in Fig. 6 for varying levels of bias above threshold. The modulation current efficiency factor was determined to be 14.2 GHz/mA$^{1/2}$. The bandwidth and resonant frequency increase as expected up to bias currents of approximately 2.5 mA and then saturate. The damping rate is also shown in Fig. 6 and parabolic fitting to the damping rate results in a damping parameter, K=0.159 ns, and initial damping constant, γ_0=18.8/ns, predicting an intrinsic bandwidth of 57 GHz.

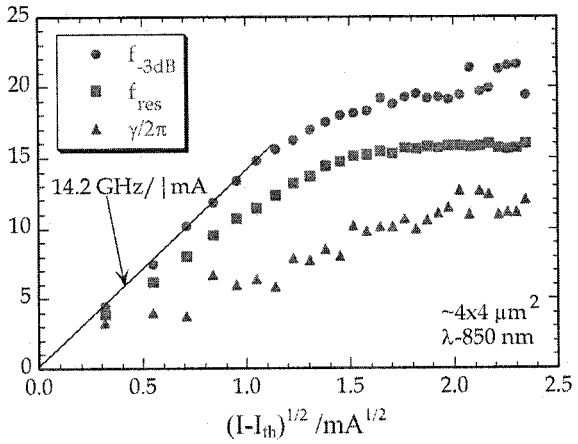

Fig. 6. 3dB bandwidth (circles), resonant frequency (squares), and damping (triangles) for the laser discussed above. Reproduced from [4].

3.3 High bandwidth 1070 nm oxide and tunnel junction VCSELs

More recent reports by Suzuki et al of NEC [8] have begun to demonstrate higher bandwidth VCSELs based on strained InGaAs quantum wells that are expected to have higher differential gain and thus higher resonance frequencies than the 850 nm devices reported by Lear et al or 780 nm devices reported by Shtengel et al. The NEC researchers have also focused on the impact that electrical parasitic circuits and thermal resistance have on maximum VCSEL bandwidth. They saw the resonant frequency of an approximately 7 μm diameter oxide confined, 1070 nm VCSEL saturating at 16 GHz, near the same value the 850 nm Sandia VCSEL reached, at a 6 mA drive current where the junction temperature rise was determined to be ΔT=30 C. The NEC VCSELs operated multimode and achieved 3dB bandwidths up to 20 GHz at bias currents of 7mA as displayed in Fig. 7. Under large signal modulation at 20 Gb/s with an extinction ratio of 5.2 dB, the VCSELs produced error rates as low as 10^{-12} for a received power of –7.7 dBm with no indication of an error floor in 5m of 50 μm core diameter, graded-index, multimode fiber. Notably, the devices could also be operated at 30 Gb/s with the same extinction ratio while displaying a clear eye opening. This is believed to be the highest reported bit rate for directly modulated VCSELs.

Suzuki et al's approach to managing thermal resistance was to increase the mesa diameter to allow additional horizontal heat flow in the epitaxial mirrors which have higher thermal conductivity than polymide planarization layers. Their data on thermal resistance of 20 and 33 μm diameter mesas are shown together with other VCSEL thermal resistance results in Fig. 12 in Section 4. To moderate the increased capacitance associated with the larger mesa, proton implants have been used which reduced the capacitance of the 33 μm diameter mesa from ~400 fF to ~130 fF. They believe that yet higher speed VCSELs are possible and that self-heating and electrical resistance continues to be an issue. Tunnel junction VCSELs where the current does not have to flow through a thick p-type DBR are being pursued to address these issues. The tunnel junction is also expected to enhance current injection uniformity [15].

3.4 Quantum dot 980 nm VCSELs

Intriguing research on VCSELs based on highly strained InGaAs material, and in particular, InAs submonolayer quantum dots (QDs)[16,17] in a GaAs host, performed by a collaboration of German institutions including Technische

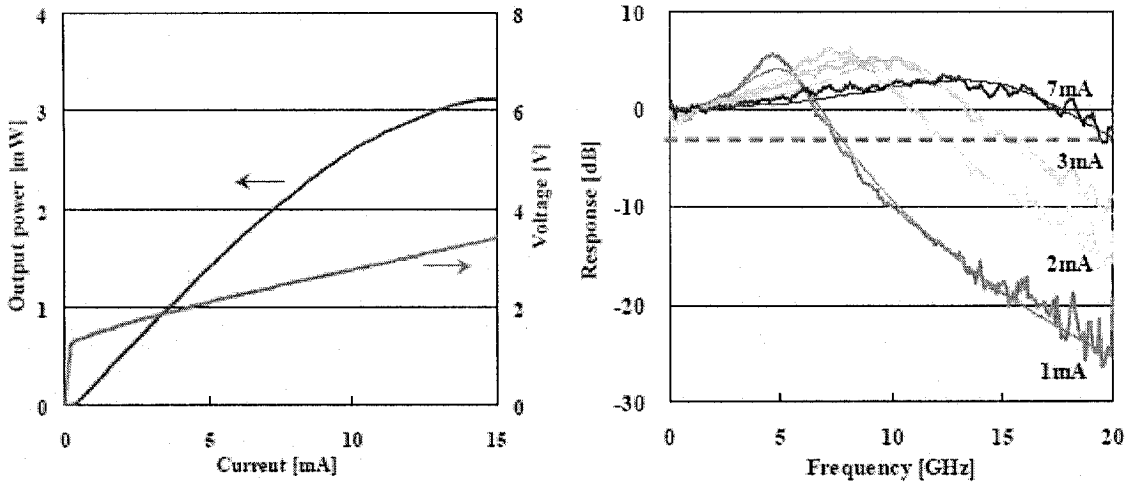

(a) (b)

Fig. 7. (a) Output power and voltage versus drive current of a high speed, 1070 nm, oxide confined VCSEL developed by NEC. (b) The measured microwave frequency response of the VCSEL at varying drive currents. Figures reproduced from [8] courtesy of N. Suzuki.

Universität Berlin, Nanosemiconductor GmbH, Heinrich-Hertz-Institut, and Max-Planck-Institut [2,18,19]. The submonolayer QD growth mechanism is an alternative to Stranski-Krastanow growth and does not require a wetting layer resulting in higher peak gain. High peak material gain is particularly important for QD VCSELs because of the reduced volume of gain material in QD lasers compared to quantum well lasers. The 980 nm devices have demonstrated high current modulation efficiency factors of 14 GHz/mA$^{1/2}$ in 1 μm active diameter single mode structures. At the highest drive levels the 3dB bandwidth falls below the resonance frequency as plotted in Fig. 8(a) indicating that RC time constants are likely limiting the device bandwidth. Fig. 8(b) shows the K-factor for the single mode QD VCSEL at low currents is K=0.24 ns corresponding to an intrinsic extrapolated bandwidth of 37 GHz, but at bias currents greater than 1 mA above threshold, the K-factor shifts to a more heavily damped K=0.57 ns. Since intrinsic resonant frequency and damping are decoupled from the electrical parasitic circuit effects as indicated in Fig. 1(b), the shift in damping may be due to thermal effects or carrier population distributions in and around the QDs.

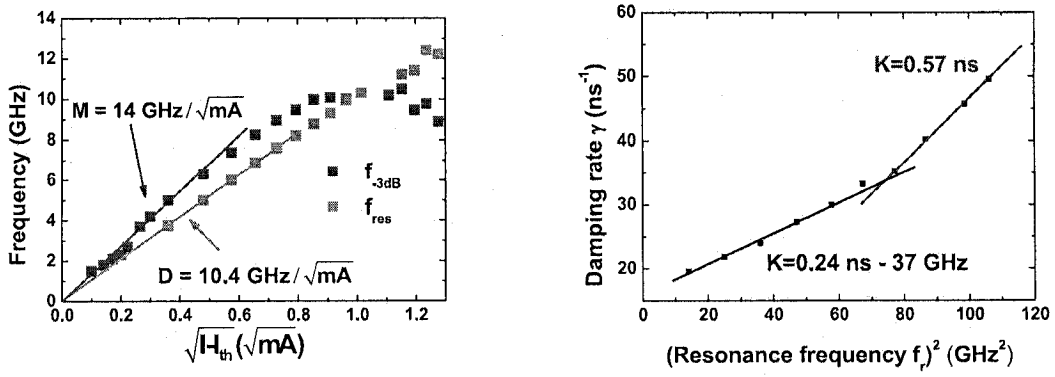

(a) (b)

Fig. 8. (a) 3dB bandwidth (blue) and resonant frequency (red) of a single mode QD VCSEL. (b) Data plot and fitting of damping rate versus the square of resonant frequency to determine the K-factor. Extrapolation of the low current K-factor indicates and intrinsic bandwidth limit of 37 GHz. Reproduced from [18,2] courtesy of F. Hopfer and A. Paraskevopoulos

Larger multimode QD VCSELs were also examined by Hopfer and collaborators [19]. The 3dB bandwidth dependence on bias current and damping rate seen in Fig. 9(a) and (b), respectively, show similar trends to the smaller single mode device. The data also supports the importance of thermal issues as the maximum bandwidth at 25 C is 15 GHz while the 85 C bandwidth falls to 13 GHz. Yet, the VCSEL is capable of operating with 20 Gb/s bit-error rates of $<10^{-12}$ at both temperatures.

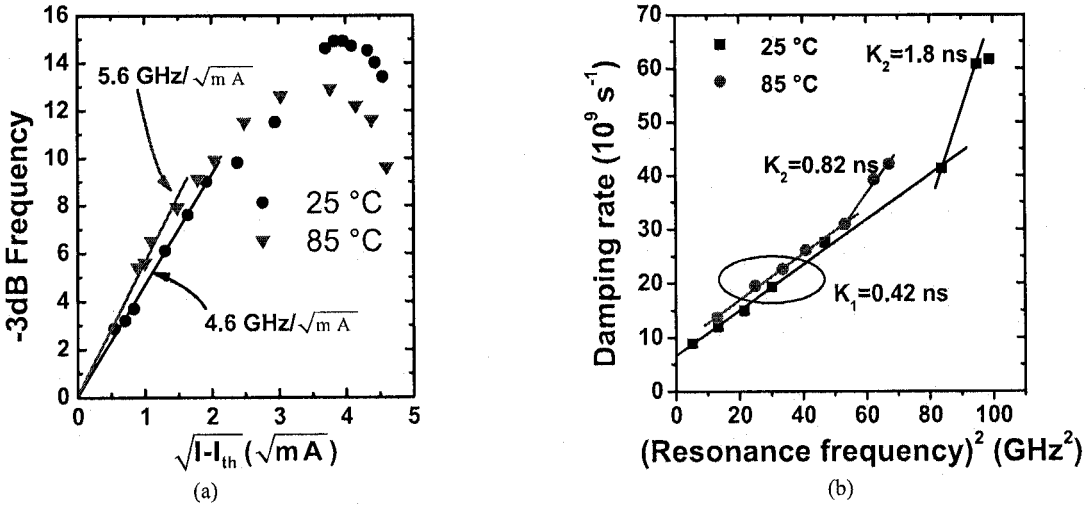

Fig. 9. 25 C and 85 C multimode QD VCSEL data for (a) 3dB bandwidth versus bias condition and (b) damping rate versus the square of resonant frequency. Reproduced from [19] courtesy of F. Hopfer.

4. NEW HIGH-SPEED VCSEL STRUCTURES

4.1 Comparison of top-emitting and bottom-emitting VCSELs for high speed operation

The preceding discussion and results have highlighted the limits that extrinsic factors place on the bandwidth of directly modulated VCSELs. In particular, consideration of the conventional top-emitting VCSEL structure shown in Fig. 10(a) indicates that its geometry inherently elevates several parameters that limit high speed operation. The annular contact requires an oxidation length that is greater than the annulus width and contact to mesa alignment tolerance if the contact does not obscure the active region. The large oxidation length contributes to mesa capacitance unless auxiliary implants are used that complicate the process and increase device resistance. The perimeter contact also contributes to spreading resistance. Together these capacitance and resistance issues contribute to larger RC time constants that can limit the electrical 3dB bandwidth for direct modulation. While some reduction in thermal resistance can be achieved by increasing the mesa size, effectively replacing very low thermal conductivity polyimide with AlGaAs, other materials can offer even better thermal conductivity. Top-emitting VCSELs are typically fabricated on GaAs substrates that are at least ~100 μm thick, placing the junction far from the backside heatsink. With respect to optical performance, the peripheral current injection of the top-emitter also leads to non-uniform current injection that favors higher order modes soon after threshold of the fundamental mode. Multimode operation decreases MCEF and overall bandwidth as discussed above.

To address the constraints imposed by the top-emitting geometry, the authors are pursuing high-speed bottom emitting VCSELs illustrated in Fig. 10(b). The disk shaped p-contact no longer needs an aperture, allowing the mesa to be about 1/3 of the diameter of top-emitting VCSEL mesas. The correspondingly shorter oxidation lengths greatly reduce mesa capacitance without requiring implants. Rather than using moderate thermal conductivity semiconductor alloys around the active region, metal can be plated around the mesa including on the sidewalls. The short oxide length allows the plated metal in close proximity to the junction, and the device can be readily mounted junction side down for yet lower thermal resistance. Results on the thermal resistance of plated copper VCSELs will be presented below. The position of the p-contact in line with the active region not only permits smaller mesas, but also results in more uniform current injection that does not promote multimode operation as much as peripheral contacts.

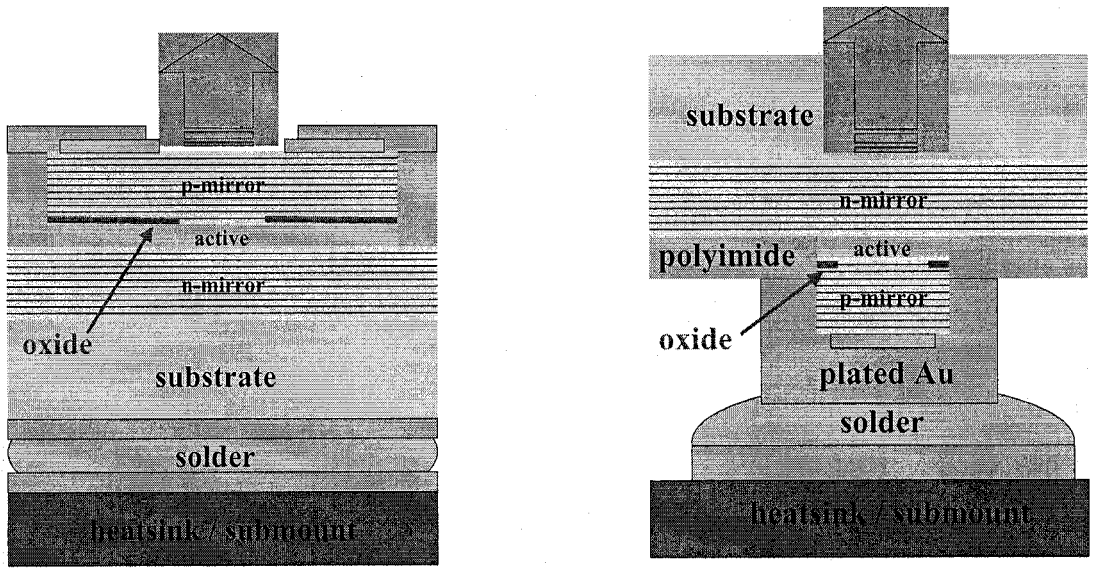

(a) (b)

Fig. 10. Cross-sectional diagrams of (a) conventional top-emitting and (b) high-speed bottom emitting VCSELs. The relative electrical, thermal, and optical benefits of the bottom-emitting structure are discussed in the text.

4.2 Plated copper heatsinks for high speed VCSELs

As prior research demonstrated the ability to increase the electrical 3dB bandwidth to values exceeding the measured modulation bandwidth, other extrinsic factors merit increased emphasis. In particular, data such as that presented in Fig. 3 and 9 highlight the need for reduced thermal resistance in VCSELs. Previously, gold plating has substantially reduced the thermal resistance of bottom-emitting VCSELs leading to increased output power[20]. The authors have pursued lower cost, slightly higher thermal conductivity copper plating, initially on top-emitting structures, to investigate the impact on modulation bandwidth[21]. Three heatsink structures shown in Fig. 11 were evaluated to understand the importance of sidewall and bottom mirror coverage. The copper plating was either restricted to the top of the mesa (Fig. 11(a)), overlapped onto the sides (Fig. 11(b)), or extended past the sidewall onto the lower mirror (Fig. 11(c)). These structures were referred to as having 0, 2, and 4 μm of overlap, respectively, based on how far the nominal opening in the photoresist that masks plating extended past the edge of the mesa. Before plating, the mesa and lower mirror were covered with a PECVD deposited 100 nm thick SiN_x layer to prevent electrically shorting the junction. Covering the sidewalls with metal substantially reduced thermal resistance compared to the 0 μm overlap case, but further extending the overlap to 4 or 6 μm gave only minor additional improvement[22]. The major effect of sidewall coverage is attributed to the anisotropic thermal conductivity of the laminar mirror structures [7,23]. Quantitative data on thermal resistance of copper plated VCSELs are presented along with data from other publications [4,20-22,24-30] in Fig. 12.

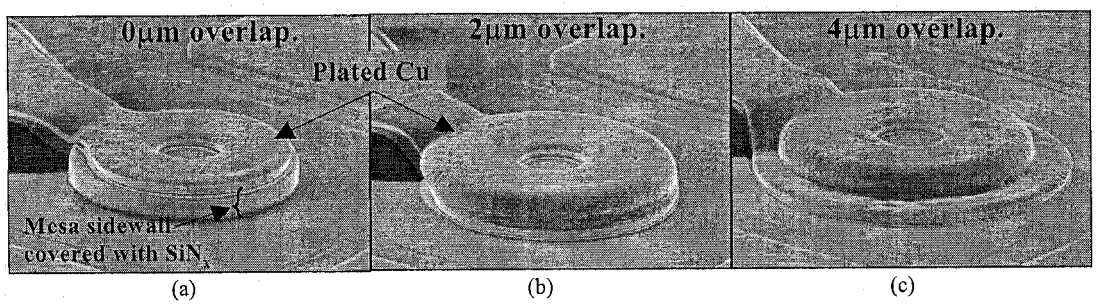

(a) (b) (c)

Fig. 11. Scanning electron microscope images of high-speed VCSELs with copper plating that nominal overlaps past the mesa (a) 0 μm, (b) 2 μm, and (c) 4 μm

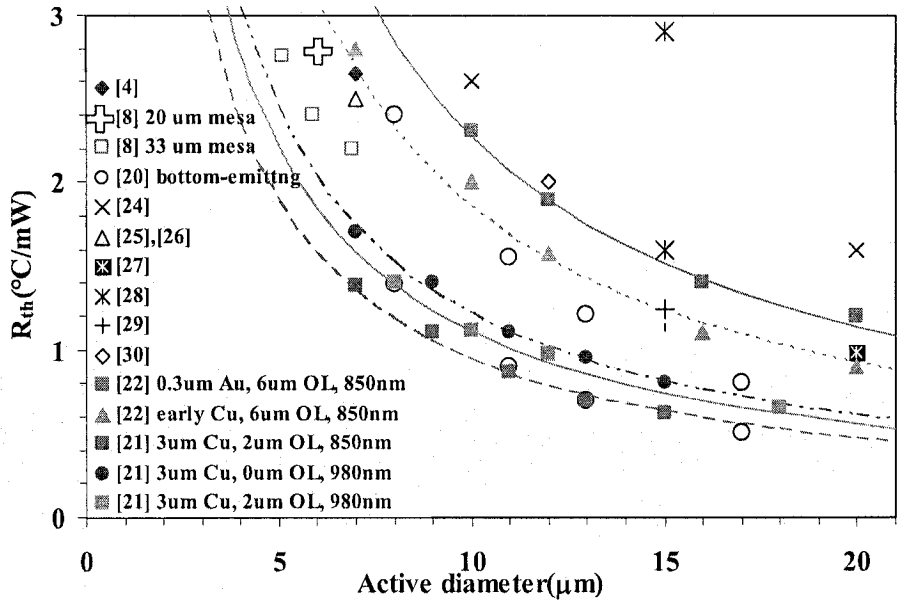

Fig. 12. Thermal resistance data from 850 nm and 980 nm top-emitting VCSELs with various overlaps (OL) of gold or copper heatsinks from the authors' work. Data from other researchers are also shown (open symbols).

One complication of the heatsink overlapping onto the mesa sidewalls and lower mirror, as seen in Fig. 13, is the additional capacitor formed across the thin SiN_x dielectric in these cases. A thicker dielectric layer would reduce the capacitance but increase the thermal resistance from the junction to the copper plating. In the earliest experiments with 300 nm evaporated gold coatings extending 6 μm beyond the mesa [22], the additional capacitance was estimated to be 240 fF from physical dimensions and parameters. The calculated electrical 3dB bandwidth for this case was 15.6 GHz and in fact the measured laser bandwidth was 16.3 GHz. However, it was determined that by restricting the overlap to 2 μm, the additional capacitance due to the heatsink could be reduced to ~94 fF, and the corresponding calculated electrical 3dB bandwidth was increased to 63 GHz, not including the mesa capacitance.

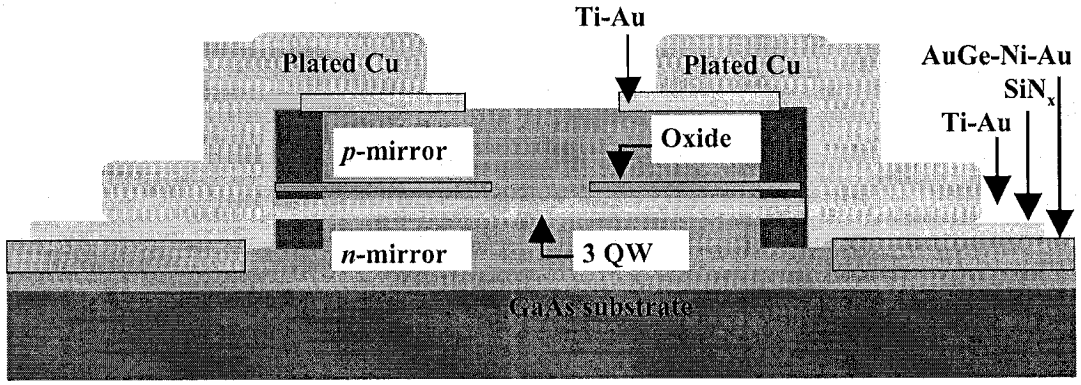

Fig. 13. Schematic cross-section of copper plated, top-emitting VCSEL.

When applied to 9 μm diameter top-emitting 980 nm VCSELs, the heatsinks with greater overlap increased the maximum output power by 130% and boosted both the MCEF from 2.2 to 5.0 GHz/$mA^{1/2}$ and maximum bandwidth from 6.1 to 9.8 GHz as seen in Fig. 14(a). Fig 14(b) shows larger heatsinks also improved the MCEF and maximum bandwidth of 850 nm lasers that were faster to begin with, but the relative improvement was smaller. Also seen in this figure is the bandwidth of larger lasers where increasing size resulted not only in smaller MCEF but also lower saturated bandwidth. The spectral data of Fig. 4, which came from the 8 μm diameter device of Fig. 14(b) indicates the likely cause is multimode operation.

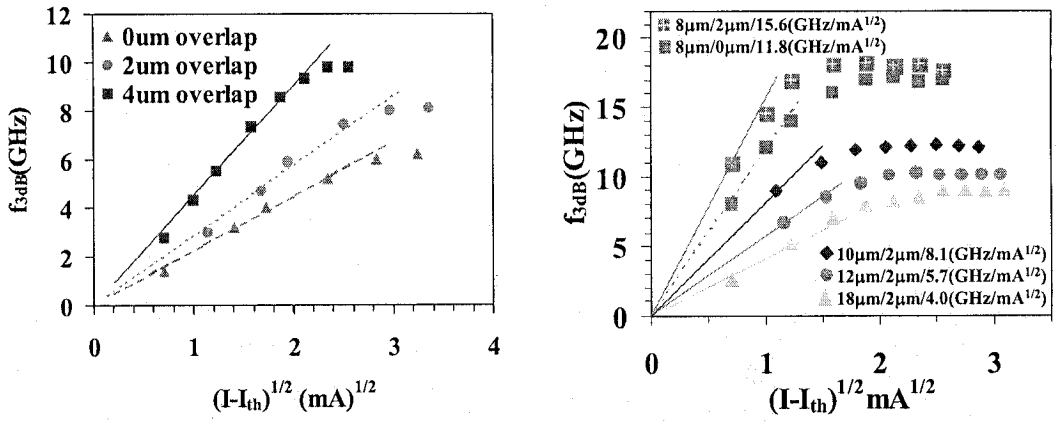

Fig. 14. 3dB bandwidth progression of (a) a moderate frequency 980 nm VCSEL and (b) a high frequency 850 nm VCSEL.

5. SUMMARY

The bandwidth of VCSELs is influenced by both intrinsic factors related to the carrier and photon dynamics as well as extrinsic factors. VCSELs have not reached the high speeds represented by their intrinsic limits but are instead constrained by electrical parasitic circuit, thermal, and mode control issues. Devices have been fabricated with electrical 3dB bandwidths in excess of 35 GHz and higher electrical limits should be possible with reduced oxide lengths and the absence of bonding or probing pads enabled by bottom-emitting geometries. Thermal issues must also be managed in order to prevent bandwidth saturation in VCSELs at high drive currents. Copper plated heatsinks have reduced thermal resistance of 10 μm diameter active region devices to approximately 1 C/mW and further improvements are possible with flip-chip bonding of bottom-emitting lasers. Mode control is now a significant issue limiting the ultimate bandwidth of these devices and will be incorporated in future high speed designs. VCSELs from multiple laboratories have now reached 3dB bandwidths of approximately 20 GHz, and 30 Gb/s modulation has been demonstrated by NEC. With further improvements in the areas described in this paper, as well as the optimization of heterostructure designs for high gain and differential gain, directly modulated 40 Gb/s VCSELs should be realized.

6. ACKNOWLEDGEMENTS

The authors gratefully acknowledge the support of DARPA under contract DAAD19-03-1-0059.

REFERENCES

[1] L. Chrostowski, X. Zhao, C.J. Chang-Hasnain, R. Shau, A. Ortsiefer, and M.C. Amann, "50-GHz optically injection-locked 1.55-mu m VCSELs", *Photonics Technology Letters*, vol. 18, pp. 367-369, 2006.
[2] A. Paraskevopoulos, "High Bandwidth VCSEL Devices", IEEE LEOS 19th Annual Meeting, Montreal, October, 2006.
[3] D. Tauber, G. Wang, R. S. Geels, J. E. Bowers, and L. A. Coldren, "Large and small signal dynamics of vertical cavity surface emitting lasers," *Applied Physic. Letters*, vol. 62, pp. 325-327, 1993.
[4] K.L. Lear, V.M. Hietala, H.Q. Hou, M. Ochiai, J.J. Banas, B.E. Hammons, J. Zolper, S.P. Kilcoyne, "Small and large signal modulation of 850 nm oxide-confined vertical cavity surface emitting lasers", *Advances in Vertical Cavity Surface Emitting Lasers* in series *OSA Trends in Optics and Photonics*, vol. 15, pp. 69–74, 1997.
[5] S. Weisser, E.C. Larkins, K. Czotscher, W. Benz, J. Daleiden, I. Esquivias, J. Fleissner, J.D. Ralston, B. Romero, R.E. Sah, A. Schonfelder, and J. Rosenzweig, "Damping-limited modulation bandwidths up to 40 GHz in undoped short-cavity In0.35Ga0.65As-GaAs multiple-quantum-well lasers", *Photonics Technology Letters*, vol. 8, pp. 608-610, 1996.
[6] A. N.AL-Omari and K. L. Lear, " Dielectric Characteristics of Spin-Coated Dielectric Films Using On-Wafer Parallel-Plate Capacitors at Microwave Frequencies," *IEEE Trans. on Diel. and Elec. Insul.*, vol. 12, no. 6, p. 1151, Dec. 2005.
[7] K.L. Lear and R.P. Schneider, "Uniparabolic mirror grading for vertical cavity surface emitting lasers", *Applied Physics Letters*, vol. 68, pp. 605-607, 1996.

[8] N. Suzuki, H. Hatakeyama, K.Yashiki, K. Fukatsu, K.Tokutome, T.Akagawa, T. Anan, and M. Tsuji, "High-speed InGaAs VCSELs", IEEE LEOS 19th Annual Meeting, paper WJ1, Montreal, Canada, October, 2006.
[9] N. Suzuki, private communication.
[10] For example, see A.S. Sedra and K.C. Smith, *MicroelectronicCircuits, 5th ed*, Oxford University Press, 2004
[11] A. N. AL-Omari, G. P. Carey, S. Hallstein, J. P. Watson, G. Dang, and K. L. Lear, "Low Thermal Resistance, Low Current Density, High-Speed 980 and 850nm VCSELs", 20th IEEE International Semiconductor Laser Conference, paper WC7, pp. 127–128, Waikoloa, Hawaii, September 17-21, 2006.
[12] F.S. Choa, Y.H. Lee, T.L. Koch, C.A. Burrus, B. Tell, J.L. Jewell, and R.E. Leibenguth, PTL "High-speed modulation of vertical cavity surface emitting lasers," IEEE Photon. Technol. Lett., vol. 3, p. 697, 1991.
[13] G. Shtengel, H. Temkin, P. Brusenbach, T. Uchida, M. Kim, C. Parsons, W.E. Quinn, and S.E. Swirhun, "High-Speed Vertical-Cavity Surface-Emitting Laser", *Photonics Technology Letters*, vol. 5, pp. 1359-1362, 1993
[14] K.L. Lear, V.M. Hietala, H.Q. Hou, M. Ochiai, J.J. Banas, B.E. Hammons, J. Zolper, S.P. Kilcoyne, "Small and large signal modulation of 850 nm oxide-confined vertical cavity surface emitting lasers", Conference on Lasers and Electro-Optics, CLEO '97, paper CWA2, vol. 11, pp.193-194, Baltimore, Maryland, May, 1997.
[15] S. Sekiguchi, T. Miyamoto, T. Kimura, G. Okazaki, F. Koyama, K. Iga, "Improvement of current injection uniformity and device resistance in long-wavelength vertical-cavity surface-emitting laser using a tunnel junction", *Japanese Journal of Applied Physics*, vol. 39, pp. 3997-4001, 2000.
[16] A.E. Zhukov, A.R. Kovsh, S.S. Mikhrin, N.A. Maleev, V.M. Ustinov, D.A. Livshits, I.S. Tarasov, D.A. Bedarev, M.V. Maximov, A.F. Tsatsul'nikov, I.P. Soshnikov, P.S. Kop'ev, Z.I. Alferov, N.N. Ledentsov, D. Bimberg, "3.9 W CW power from sub-monolayer quantum dot diode laser," *Electronics Letters*, vol. 35, pp. 1845-1847, 1999.
[17] S. S. Mikhrin, A.E. Zhukov, A.R. Kovsh, N.A. Maleev, V.M. Ustinov,Y.M. Shernyakov, I.P. Soshnikov, D.A. Livshits, I.S. Tarasov, D.A. Bedarev, B.V. Volovik, M.V. Maximov, A.F. Tsatsul'nikov, N.N. Ledentsov, P.S. Kop'ev, D. Bimberg, Z.I. Alferov, "0.94 mu m diode lasers based on Stranski-Krastanow and sub-monolayer quantum dots", *Semicond. Sci. Technol.* 15, p. 1061-1064, 2000.
[18] F. Hopfer, I. Kaiander, A. Lochmann, A. Mutig, S. Bognar, M. Kuntz, U.W. Pohl, V.A. Haisler, D. Bimberg, "Single-mode submonolayer quantum-dot vertical-cavity surface-emitting lasers with high modulation bandwidth", *Applied Physics Letters*, vol. 89, ID: 141106, 2006.
[19] F. Hopfer, A Mutig, G.Fiol, M.Kuntz, V.Shchukin, N.N.Ledentsov, D.Bimberg, S.S.Mikhrin, I.L.Krestnikov, D.A.Livshits, A.R.Kovsh, and C.Bornholdt, "20 Gb/s 85 °C Error Free Operation of VCSEL based on Submonolayer Deposition of Quantum Dots", 20th IEEE Int'l Semiconductor Laser Conf., pp. 119-120, Hawaii, September, 2006.
[20] T. Wipiejewski, D.B. Young, M.G. Peters, B.J. Thibeault, L.A. Coldren, "Improved Performance of Vertical-Cavity Surface-Emitting Laser-Diodes with Au-Plated Heat Spreading Layer", *Electronics Letters*, vol. 31, pp. 279-281, 1995.
[21] A.N. Al-Omari, G.P. Carey, S. Hallstein, J.P. Watson, G. Dang, K.L. Lear, "Low Thermal Resistance, High Speed, Top Emitting 980nm VCSELs," *Photonics Technology Letters*, vol. 18, no. 11, pp.1225- 1227, 2006.
[22] A. N. AL-Omari and K. L. Lear, "VCSELs with a Self-Aligned Contact and Copper-Plated Heatsink", *Photonics Technology Letters*, vol. 17, no. 9, pp. 1767 - 1769, Sept. 2005.
[23] G. Chen, C.L. Tien, X. Wu, and J.S. Smith, "Thermal-diffusivity measurement of GaAs/AlGaAs thin-film structures", *Journal of Heat Transfer of the ASME*, vol. 116, pp. 325-331, 1994.
[24] A. N. AL-Omari and K. L. Lear, "Polyimide-Planarized Vertical-Cavity Surface Emitting Lasers with 17.0 GHz Bandwidth," IEEE Photonics Technology Letters, vol. 16, 969-971, 2004.
[25] K. D. Choquette, R. P. Schneider, K. L. Lear, and K. M. Geib, "Low threshold voltage vertical-cavity lasers fabricated by selective oxidation," IEE Electronics Letters, vol. 30, p. 2043, Nov. 1999.
[26] B.J. Thibeault et al., "High speed characteristics of low optical loss oxide apertured vertical cavity lasers," IEEE Photonics Technology Letters, vol. 9, pp. 11-13, Jan. 1997.
[27] D. L. Mathine, H. Nejad, D. R. Allee, R. Droopad, and G. N. Maracas, "Reduction of the thermal impedance of vertical-cavity surface-emitting lasers after integration with copper substrates," *Appl. Phys. Lett.*, vol. 69, p. 463, 1996.
[28] S. Matsuo, T. Nakahara, K. Tateno, H. Tsuda, and T. Kurokawa, "Hybrid integration of smart pixel with vertical cavity surface emitting laser using polyimide bonding," *OSA Trends in Optics and Photonics*, vol. 14, p.39,1997.
[29] R. Pu, C. W. Wilmsen, K. M. Geib, and K. D. Choquette, "Thermal resistance of VCSELs bonded to integrated circuits," IEEE Photonics Technology Letters, vol. 11, pp. 1554-1556, Dec. 1999.
[30] T. Wipiejewski, D. B. Young, B. J. Thibeault, and L. A. Coldren, "Thermal crosstalk in 4×4 vertical-cavity surface-emitting laser arrays," IEEE Photonics Technology Letters, vol.8, pp.980 – 982, Aug. 1996.